Optimal Capacitor Planning for Power Factor Improvement Using Hybrid Particle Swarm and Harmony Search Optimization

A. H. Ibrahim[1], E. C. Ashigwuike[2], W. Oluyombo[3], A. A. Sadiq[4*]
[1]Hydroelectric Power Producing Areas Development Commission
[2, 3] University of Abuja Nigeria
[4]Federal University of Technology, Minna

ABSTRACT: Industrial loads reduce the Power Factor (PF) of supply systems, causing increases in power losses, damaging equipment and higher utility bills. Optimization techniques are used in planning reactive sources to improve PF of power systems. However, conventional techniques suffer difficulties in passing over local optimal, divergence risk, constraints handling or computing higher order derivatives. Herein, the hybridization of Particle Swarm and Harmony Search Algorithm (PS – HSA) is developed for optimal capacitor planning to improve PF, and comparison is made with the Enhanced Particle Swarm Optimization (EPSO) and Improved Adaptive Harmony Search Algorithm (IAHSA). The test systems are the Modified IEEE 6 and 16 buses and nodes respectively. To create semblance of industrial load dominated power systems, the test networks were modified by increasing the reactive load demand at all buses of the IEEE 6 and 16 by 50% and 70% respectively. The capacitor is modelled as static shunt-controlled element deployed to inject reactive power at buses/nodes. Results show that for IEEE 6 buses, PF improved from 0.68 to 0.8983, 0.8986 and 0.8992 with EPSO, IAHSA and hybrid PS – HSA respectively. Similarly, in IEEE 16 nodes, PF improved from 0.76 to 0.9439, 0.943, and 0.944 with EPSO, IAHSA and hybrid PS – HSA respectively. Furthermore, real power losses reduced from 16.94 MW to 14.03 MW in IEEE 6 buses, translating to 17.2% reduction with the hybrid PS - HSA. While in IEEE 16 nodes, reduction is from 0.719 MW to 0.69 MW accounting for 4% reduction, also with the hybrid PS - HSA.

KEYWORDS: Power Factor, Capacitor, Particle Swarm Optimization, Harmony Search Algorithm, Power losses

[Received June 8, 2023; Revised July 31, 2023; Accepted Aug. 7, 2023] Print ISSN: 0189-9546 | Online ISSN: 2437-2110

I. INTRODUCTION

An electrical power system is responsible for supplying electrical power to various types of electrical loads, including resistive, capacitive, and inductive loads (Beck, 2018). Each load type exhibits distinct electrical characteristics when connected to the power system. A resistive load converts electrical energy into thermal energy and consumes power in such a way that the current wave remains in sync with the voltage wave. Hence, the Power Factor (PF) for a resistive load is unity. On the other hand, a capacitive load causes the current wave to lead the voltage wave due to the time required for the dielectric material to charge up fully. Consequently, the PF of a capacitive load is leading. Similarly, an inductive load causes the current wave to lag behind the voltage wave as it takes time to establish its magnetic field when voltage is applied. Therefore, the PF of an inductive load is lagging (Blume, 2007; Che Soh *et al*., 2014). The PF in an electrical power system is defined as the cosine of the angle between the current and voltage (Che Soh *et al*., 2014).

Due to the inherent characteristics of inductive loads, it leads to reduced PF in an electrical power system (Subjak and Mcquilkin, 1990). Work in García *et al*., (2003) and Lasseter *et al*., (2011) opined that one of the factors that causes inefficiencies in electrical power system is PF, and leads to loss in power system. Also, Lasseter *et al*., (2011) and Che Soh *et al*., (2014) indicated that inductive loads such as induction motors, transformers, ballast lamps, welding machine, induction furnace, causes low power factors in power system, because when inductive loads are connected to electrical power system, it draws magnetizing current to maintain magnetic field of coils and this magnetizing current is out of phase with voltage. The magnetizing current, responsible for generating flux in the iron, operates out of phase with the voltage and induces rotation in the motor shaft. This current remains unaffected by the load driven by the motor and typically ranges from 20% to 60% of the rated full load current (Lasseter *et al*., 2011). However, the magnetizing current does not contribute to the work output of the inductive load. Consequently, when dealing with an inductive load with a magnetizing current equivalent to 25% of the full rated current, the power factor of the electrical power system decreases to 0.75, thereby reducing the overall efficiency of the system to 75%.

The inefficiencies of electrical power system introduced by low PF; power factor correction becomes very important in electrical power systems. Improving PF reduces loss in the electrical power system as the effect of magnetizing current

*Corresponding author: ahmad.abubakar@futminna
doi: http://dx.doi.org/10.4314/njtd.v18i4.2

(reactive power) of inductive loads are reduced while not affecting the operation of the inductive loads. In all PF correction techniques, the goal is to inject a leading current into the electrical power system to cancel the effect of lagging current introduced by the inductive loads. The power factor is improved basically by connecting devices that have the capacity to draw leading power in parallel with the load drawing lagging power, thus partly or completely neutralizing the lagging power component of the load and thereby improving the power factor of the system.

Reactive current in the transmission system contributes to increased losses, reduced power factor, decreased power transmission capacity, and potential voltage fluctuations at the receiving end. Additionally, abrupt variations in reactive power consumption by inductive loads can induce voltage amplitude oscillations, which can impact the real power demand of the electric system and give rise to power oscillations (Mehta and Mehta, 2008; Ospina and Van Cutsem, 2020). Because load connected in an electrical power system is not static, dynamic method of power factor correction is the best method for improving the power factor of electrical power system. Capacitors are used in correcting power factor in electrical power system as it injects leading current into the electrical power system, thereby countering the effect of the lagging current caused by inductive load. Optimal correction of power factor requires that a power factor close to unity is achieved, in which voltage and current in the electrical power system are in phase, or in order words, the lagging current caused by inductive load is of the same magnitude and in opposite direction to the leading current injected by capacitor into the electrical power system. If the capacitor connected to the electrical system injects less leading current than the lagging current into the electrical power system, the resultant power factor will be less than 1 while injecting high leading current into the system by using higher capacitance value leads to over correction of the power factor, making the power factor more than 1, which introduces more problem in the power system.

Conventional approaches to capacitor planning are based on discrete allocation of the capacitor banks, and the reactive power injection from a capacitor bank is also discrete. For instance, the loss sensitivity factors is used to identify the buses requiring compensation in (Elsheikh *et al*., 2014), while some voltage stability indices are used to determine the optimal buses aimed at improving power factor in (Sajjadi, Haghifam and Salehi, 2013; Gampa and Das, 2016). Recently, optimization algorithms such as Particle Swarm Optimization (PSO) and their enhance variants were deployed for capacitor planning to improve power factor (Tahir, Rasheed and Rahmat, 2022). The PSO approach and its variant are however deficient in exploitation capability compare to exploration, which makes them vulnerable to local optimal solution.

PSO deploys multiple candidate solution refers to as particles over the entire search space. The candidate solutions co-exist and cooperates simultaneously. Each particle of the swarm flies in the entire search space, which improves the exploration capability of PSO over its exploitation of given solution space. On the other hand, the Harmony Search Algorithm's (HAS), implementation has capability in improving exploitation with few adjustable parameters, easy and the ability to balance exploitation and exploration during search. This paper therefore, developed a hybrid which aims to enhance the exploitation capability of PSO by through hybridization of PSO with the Harmony Search Algorithm (HSA).

Brief Review

Ramadan, *et al.*, (2017) utilizes PSO to address the capacitor allocation problem in power distribution systems, specifically a modified IEEE 16-nodes distribution system connected to wind power generation. Through proper capacitor allocation and optimization, they achieved reductions in power losses and improvements in the voltage profile while ignoring power factor correction. Also, Eswaran and Kumar, (2017) utilized PSO to identify optimal turning point for distributed static synchronous compensator (DSTATCOM) for controlling reactive power demand in both distributed power management systems and grid-connected systems without power factor correction. In another view point, Mohammadi, (2017) employed a PSO algorithm to simultaneously determine the optimal placement and sizing of a shunt Active Power Conditioner (APC) and shunt capacitor in a distribution system with harmonic distortion. The objective function considered were power losses, energy losses, and the costs associated with capacitor banks and APCs. In a similar vein, Yapici and Çetinkaya, (2017) proposed the Eagle Strategy with Particle Swarm Optimization (ESPSO) to improve the efficiency of PSO for minimizing power losses in power systems. In contrast, Bouaraki and Recioui, (2017) utilized Teaching Learning Based Optimization for the optimal placement of power factor correction capacitors in power systems, the optimization was tested on distribution network only.

In Mendoza, *et al.*, (2019), optimal capacitor allocation and sizing in distribution networks using PSO algorithm was demonstrated, while Neupane *et al.*, (2020), also utilizes PSO to obtain only the optimal sizes of capacitors and the optimal location was obtained using Loss Sensitivity Factors; an approach vulnerable of local optimal solutions with false loss sensitivity location. Again, the approach was demonstrated in 33-kV distribution system, and the performance in transmission network is uncertain. Balu and Mukherjee, (2020) employed Constriction Factor Particle Swarm Optimization (CFPSO) to determine the optimal location and sizing of Distributed Generation and Shunt Capacitor Banks in a radial distribution system, with power loss, stabilized voltage profile, increased the system stabilization index and voltage deviation IEEE 33-bus system, thus outperforming traditional PSO. In another variant of PSO, Zou, (2021) developed a fuzzy PSO for reactive power optimization control without considering impacts on power factor.

Consequently, Iza, *et al.*, (2022) focused on power factor improvement by employing conventional PSO for the optimal planning of D-STATCOM; Kumar, (2022) uses the fuzzy-PSO to enhance power quality in a photovoltaic integrated shunt active power filter; Chen, *el al.*, (2022) demonstrated the optimal allocation of capacitor banks in distribution systems

using PSO that incorporated time-varying acceleration coefficients. While the fuzzy-PSO variants is promising, the discrete nature of fuzzy decisions is also vulnerable to local optimal and thus unable to provide a balance between exploration and exploitation especially in convex and mix-integer optimization problems. Hence, to improve the exploitation ability of PSO, Tahir, *et al.,* (2022) uses an Enhanced Modified Particle Swarm Optimization approach for optimal placement of capacitors in radial distribution grids while the robustness in transmission networks with higher power flow and stressed voltages were not considered.

The studies reviewed thus far above, employ PSO or its variants as an optimization algorithm to solve different optimization problems in power systems. Particularly, PSO is utilized for optimal single capacitor allocation, sizing, and placement, as well as for achieving power loss reduction, voltage profile enhancement, reactive power demand management, power factor improvement, and optimal allocation of capacitor banks (Gampa and Das, 2016; Balu and Mukherjee, 2020; Tahir, Rasheed and Rahmat, 2022). These studies demonstrate the effectiveness of PSO in addressing various optimization challenges only in power distribution systems, while also ignoring the performance of these approaches in the transmission network. Moreover, none of the variants of PSO improves its exploitation capability.

Therefore, Qiao, *et al.,* (2015) employed an Adaptive Particle Swarm Optimization (APSO) for Reactive Power Optimization (RPO), enhancing convergence rate and accuracy. The algorithm was validated on the IEEE 30-bus power system. In a different study, Khadhraoui *et al.*, (2016) utilized a Modified Particle Swarm Optimization (MPSO) to optimize component selection for shunt active filters, aimed at harmonic elimination and power factor correction. The MPSO algorithm facilitated the identification of optimal control parameter values for a given load. Naderi *et al.*, (2017) presented a Fuzzy Adaptive Heterogeneous Comprehensive-Learning Particle Swarm Optimization (FAHCLPSO) algorithm for addressing the large-scale Optimal Reactive Power Dispatch (ORPD) problem in transmission networks to minimize active power losses and voltage deviation. In Hussain, *et al.,* (2018), the MPSO is applied for Reactive Power Dispatch (RPD). The MPSO resulted in improved search quality, reduced calculation time, and enhanced convergence characteristics. Furthermore, Yoshida and Fukuyama, (2018) introduced Differential Evolution Particle Optimization for voltage and reactive power control in transmission. The proposed algorithm improved solution quality and computation speed, outperforming conventional techniques in terms of active power loss minimization. Lotfi, *et al.,* (2018) focused on simultaneous placement of capacitors and distributed generation (DG) in distribution networks using PSO algorithm, aiming to optimize the system's performance.

Although, PSO were applied for optimizing different objectives in power systems, these studies showcase the application of PSO to address optimization problems performing well in either distribution or transmission networks of a power systems. However, the exploitation capability in terms of ability to exhaustively search a given space in contrast to the entire search space, has not been adequately addressed. This is evident from the focus of these studies on either distribution or transmission networks only. Thus, the conventional PSO and its variants still suffer from issues of local optimal due to lack of balance between exploration and exploitation capability. Researchers have also introduced variants of the PSO such as Fuzzy control based PSO, Adaptive PSO, Enhanced PSO, Improved PSO, Comprehensive learning PSO, Improved Pseudo-Gradient Search-Particle Swarm Optimization (IPG-PSO), Eagle Strategy with PSO (ESPSO), Modified PSO (MPSO), and Constriction Factor PSO (CFPSO) to optimize different objectives in power systems, achieving notable improvements in terms of active power loss minimization, convergence rate, accuracy, and overall system performance. However, these variants are limited in improving the exploitation capacity of the conventional PSO.

Consequently, this paper develops a hybrid Particle Swarm and Harmony Search Algorithm (PS – HSA) for power factor correction in a reactive load dominated power systems. The developed PS – HSA was demonstrated in both transmission and distribution network. The rest of the paper is systematically organized thus: Section II provide formulation of load flow equation for the power flow routine, problem formulation and methodology are described in section III, results and their discussion is presented in section IV and section V draws conclusion from the results obtained.

II. FORMULATION OF LOAD FLOW EQUATIONS

Generally, the complex power flow equation with real coefficients is given by Eqn. (1).

$$S_i = V_i I_i = V_i \left(\sum_{k=1}^{n} Y_{ik} V_k \right)^* = V_i \sum_{k=1}^{n} Y_{ik}^* V_k^* \qquad (1)$$

In Eqn.(1), $S_i, V_i, V_{k,} I_i \text{ and } Y_{ik}$ are the apparent power, voltage magnitude at ith and kth buses, as well as the admittance between ith and kth buses respectively.

The admittances, complex voltages at the ith and kth buses and voltage angles are defined by Eqns. (2) to (4) respectively.

$$Y_{ik} = G_{ik} + jB_{ik} \qquad (2)$$

$$V_i = |V_i| e^{j\theta_i} = |V_i| \angle \theta_i \qquad (3)$$

$$\theta_{ik} = \theta_i - \theta_k \qquad (4)$$

The complex power equation described in Eqn (5) is resolved into the real and reactive power to obtain the power balance Eqns. (6) and (7).

$$S_i = P + jQ_i = V_i \sum_{k=1}^{n} Y_{ik}^* V_k^* = \sum_{k=1}^{n} |V_i||V_k| e^{j\theta_{ik}} \left(G_{ik} - jB_{ik} \right)$$

$$= \sum_{k=1}^{n} |V_i||V_k| \left(\text{Cos}\,\theta_{ik} + j\,\text{Sin}\,\theta_{ik} \right) \left(G_{ik} - jB_{ik} \right) \qquad (5)$$

$$P_i = P_{Gi} - P_{Di} = \sum_{k=1}^{n} |V_i||V_k| \left(G_{ik}\,\text{Cos}\,\theta_{ik} + B_{ik}\,\text{Sin}\,\theta_{ik} \right) \qquad (6)$$

$$Q_i = Q_{Gi} - Q_{Di} = \sum_{k=1}^{n} |V_i||V_k|\left(G_{ik}\,\mathrm{Sin}\,\theta_{ik} - B_{ik}\,\mathrm{Cos}\,\theta_{ik}\right) \tag{7}$$

In the Newton-Raphson power flow algorithm, the Newton's method is used to determine the voltage magnitude and angle at each bus in the power system that satisfies power balance of Eqns. (6) and (7). Therefore, the task here is to solve the power balance equations such that we have Eqns. (8) and (9).

$$\sum_{k=1}^{n} |V_i||V_k|\left(G_{ik}\,\mathrm{Cos}\,\theta_{ik} + B_{ik}\,\mathrm{Sin}\,\theta_{ik}\right) - P_{Gi} + P_{Di} = 0 \tag{8}$$

$$\sum_{k=1}^{n} |V_i||V_k|\left(G_{ik}\,\mathrm{Sin}\,\theta_{ik} - B_{ik}\,\mathrm{Cos}\,\theta_{ik}\right) - Q_{Gi} + Q_{Di} = 0 \tag{9}$$

For convenience, Eqns. (6) and (7) is written as in Eqns. (10) and (11), while the simplified power balance equation is expressed in Eqns. (12) and (13).

$$P_i(\mathrm{X}) = \sum_{k=1}^{n} |V_i||V_k|\left(G_{ik}\,\mathrm{Cos}\,\theta_{ik} + B_{ik}\,\mathrm{Sin}\,\theta_{ik}\right) \tag{10}$$

$$Q_i(\mathrm{X}) = \sum_{k=1}^{n} |V_i||V_k|\left(G_{ik}\,\mathrm{Sin}\,\theta_{ik} - B_{ik}\,\mathrm{Cos}\,\theta_{ik}\right) \tag{11}$$

$$P_i(\mathbf{x}) - P_{Gi} + P_{Di} = 0 \tag{12}$$

$$Q_i(\mathbf{x}) - Q_{Gi} + Q_{Di} = 0 \tag{13}$$

In Eqns. (12) and (13), the terms $P_i(\mathbf{x})$ and $Q_i(\mathbf{x})$ expresses power flow from the ith bus into the system and represented in terms of voltage magnitudes and angles, while P_{Gi} P_{Di}, Q_{Gi}, Q_{Di} are the generations and demand at the given bus.

In a system consisting of a slack bus and the remaining PQ buses, the power flow problem entails utilizing the power balance equations to determine the unknown voltage magnitudes and angles based on the provided bus generations and demands. Subsequently, the obtained solution is utilized to calculate the real and reactive power injection at the slack bus.

Assume the slack bus is the first bus (with a fixed voltage angle/magnitude). The goal therefore is to determine the voltage angle/magnitude at the other buses. Consequently, the compact power flow Eqn. (14) is solved, with the definitions given by Eqns. (15) and (16).

$$f(\mathrm{X}) = 0 \tag{14}$$

$$\mathrm{X} = \begin{bmatrix} \theta_2 \\ \vdots \\ \theta_n \\ |V_2| \\ \vdots \\ |V_n| \end{bmatrix} \tag{15}$$

$$f(\mathrm{X}) = \begin{bmatrix} P_2(\mathrm{X}) - P_{G2} + P_{D2} \\ \vdots \\ P_n(\mathrm{X}) - P_{Gn} + P_{Dn} \\ Q_2(\mathrm{X}) - Q_{G2} + Q_{D2} \\ \vdots \\ Q_n(\mathrm{X}) - Q_{Gn} + Q_{Dn} \end{bmatrix} \tag{16}$$

The Jacobian elements are calculated by differentiating each function, $f_i(\mathrm{X})$, with respect to each variable. A typical Jacobian is given by Eqn. (17).

$$J(\mathrm{X}) = \begin{bmatrix} \frac{\partial f_1}{\partial x_1}(\mathrm{X}) & \frac{\partial f_1}{\partial x_1}(\mathrm{X}) & \cdots & \frac{\partial f_1}{\partial x_{2n-2}}(\mathrm{X}) \\ \frac{\partial f_2}{\partial x_1}(\mathrm{X}) & \frac{\partial f_2}{\partial x_1}(\mathrm{X}) & \cdots & \frac{\partial f_2}{\partial x_{2n-2}}(\mathrm{X}) \\ \vdots & \ddots & \ddots & \vdots \\ \frac{\partial f_{2n-2}}{\partial x_1}(\mathrm{X}) & \frac{\partial f_{2n-2}}{\partial x_1}(\mathrm{X}) & \cdots & \frac{\partial f_{2n-2}}{\partial x_{2n-2}}(\mathrm{X}) \end{bmatrix} \tag{17}$$

A. MVAR Estimation of Capacitors

The reactive power injection from a capacitor bank, in order to improve power factor from a given value pf_1 to a target value pf_2 is approximately estimated by Eqn. (18), where Q_c is the total injective reactive power of the capacitor bank, θ_1 and θ_2 are the inverse cosine of the power factor (pf) values of a given and targeted values respectively.

$$Q_c = P_G(\tan\theta_1 - \tan\theta_2) \tag{18}$$

$$\theta_1 = \cos^{-1} pf_1 \tag{19}$$

$$\theta_2 = \cos^{-1} pf_2 \tag{20}$$

Eqn. (21) defines the total real power generation of the test network under consideration and whose power factor is to be improved.

$$P_G = \sum_{i=1}^{ng} P_g^i \tag{21}$$

Thus, in the reactive power estimation of Eqn. (18), the total network's real power generation is computed by Eqn. (21),while Eqns. (19) and (20) gives the inverse cosine of the power factors before and after reactive compensation.

III. METHODOLOGY AND PROBLEM FORMULATION

A. Simulation Environment MATLAB/MATPOWER

The simulation environment involves the exchange of data and information between MATPOWER which executes the load flow (thereby computing the power factor, power losses and voltage) and the MATLAB which implement the optimization routines of (IAHSO and E-PSO). Figure 1 illustrate the implementation and information exchange between MATPOWER and MATLAB.

Firstly, the load flow solution at base case obtained from MATPOWER routines provides the power factor, power loss and voltage deviation without capacitor compensation. This generated data is passed into the MATLAB which runs the optimization algorithms. In the initialization of PSO and HSA, initial random solutions comprising of capacitor locations and sizes, this information are also passed into the MATPOWER load flow routine to evaluate the fitness: power factor, power loss and voltage deviation with the capacitor compensation. This bidirectional information exchange continues until the stopping criteria.

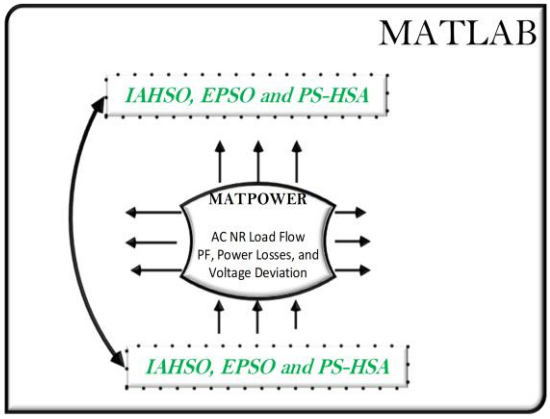

Figure 1: Schematic of Data Exchange in the implementation environment

B. Formulation of Objective function for Power Factor Correction

The power factor correction techniques adopted is the optimal capacitor placement and sizing using metaheuristic optimization. The objective is the maximization of the power factor of inductive load dominated power system. From the p-q transformation theory, the active and reactive power of electrical system is given by Eqns. (22) and(23).

$$p = v_\alpha i_\alpha + v_\beta i_\beta \tag{22}$$

$$q = v_\alpha i_\beta - v_\beta i_\alpha \tag{23}$$

Where p and q are the active and reactive powers respectively. Where vα and iα are real voltage and current value, while vβ and iβ are T/4 period delayed value from voltage and current data which will be obtained from T/4 delay orthogonal signal generator (OSG).

The power factor of the electrical system can be determined using Eqns. (24) to (27).

$$Apparent\ power\ (S) = \sqrt{p^2 + q^2} \tag{24}$$

$$Power\ \ factor(pf) = \frac{p}{S} \tag{25}$$

$$pf = \frac{p}{\sqrt{p^2 + q^2}} \tag{26}$$

$$pf = \frac{v_\alpha i_\alpha + v_\beta i_\beta}{\sqrt{(v_\alpha i_\alpha + v_\beta i_\beta) + (v_\alpha i_\beta - v_\beta i_\alpha)}} \tag{27}$$

For a given power systems network with n_g number of generators, the power factor of the entire network is calculated from the source end according to Eqn. (28). Where P_g^i and S_g^i are the i[th] generator's active and apparent power generation (Mahmoud and Emam, 2022).

$$pf = \sum_{i=1}^{n_g} \frac{P_g^i}{S_g^i} \tag{28}$$

Hence, the optimal capacitor planning in a reactive power dominated power systems seeks to optimally determine the location and amount of MVAR injection to improve the power factor (B. -J. Huang, 2018; Prasetyo *et al.*, 2021).

C. Modelling of Capacitors in Load Flow

Shunt capacitors are static controlled elements deployed to inject reactive power at buses whose voltage magnitude fall below or above the acceptable voltage range. The shunt capacitor is often installed at the load nodes in a transmission and distribution substation, along the distribution feeder, or in a transmission substation. The shunt capacitor is modeled as a fixed impedance to ground at a bus given as bus i (Qin *et al.*, 2019). The admittance of the shunt capacitor element at bus i is given by the Eqn. (29).

$$y_{sh}^i = g_{sh}^i + jb_{sh}^i \tag{29}$$

An $n_b \times 1$ vector of shunt admittances at all buses of a network is expressed by Eqn. (30).

$$Y_{sh} = G_{sh} + jB_{sh} \tag{30}$$

In MATPOWER, the parameters g_{sh}^i and b_{sh}^i are specified in columns ***GS (5)*** and ***BS (6)***, respectively, in the i[th] row of the bus matrix as equivalent MW (consumed) and MVAr (injected) at a nominal voltage magnitude of 1.0 p.u., and angle of zero (Zimmerman, *et al.* (2011).

Figure 2 depicts the simple model of a shunt capacitor connected at a bus bar for power factor correction.

The power flow equations (in terms of the active and reactive components) for a power system network without capacitor compensation, solved by Newton-Raphson's iterative method are expressed by Eqns. (31) and (32).

$$P_i^g - P_i^d = \sum_{j=1}^{n} \left| V_i V_j Y_{ij} \right| \text{Cos}(\theta_{ij} + \delta_j - \delta_i) \quad i = 1, 2, 3 \cdots n \tag{31}$$

$$Q_i^g - Q_i^d = -\sum_{j=1}^{n} \left| V_i V_j Y_{ij} \right| \text{Sin}(\theta_{ij} + \delta_j - \delta_i) \quad i = 1, 2, 3 \cdots n \tag{32}$$

Where active and reactive power generated at the i[th] bus are P_i^g and Q_i^g respectively. Active and reactive power consumed at the i[th] bus are P_i^d and Q_i^d. $V \angle \delta$ is the bus voltage and associated angle, $Y_{ij} \angle \theta$, denotes the element of bus admittance matrix and the associated angle. Applying Taylor series to Eqns. (31) and (32), the following first order approximation is obtained as Eqn. (33).

$$\begin{bmatrix} \Delta P \\ \Delta Q \end{bmatrix} = \begin{bmatrix} J_1 & J_2 \\ J_3 & J_4 \end{bmatrix} \begin{bmatrix} \Delta \delta \\ \Delta |V| \end{bmatrix} \tag{33}$$

The active and reactive power mismatch is thus expressed in Eqns. (34) and (35).

$$\Delta P_i^{(k)} = P^{sch} - P_i^{(k)} \tag{34}$$

$$\Delta Q_i^{(k)} = Q^{sch} - Q_i^{(k)} \tag{35}$$

From the Eqns. (34) and (35), The new estimate for bus voltages is expressed by Eqns. (36) and (37).

$$\delta_i^{k+1} = \delta_i^{(k)} + \Delta \delta_i^{(k)} \tag{36}$$

$$V_i^{k+1} = \left| V_i^{(k)} \right| + \Delta \left| V_i^{(k)} \right| \tag{37}$$

Now, with the injection of reactive power from the shunt-connected capacitor, the reactive power Eqn. (32) becomes modified and expressed by Eqn. (38).

$$Q_i^g - Q_i^d + Q_i^c = -\sum_{j=1}^{n} \left| V_i V_j Y_{ij} \right| \text{Sin}(\theta_{ij} + \delta_j - \delta_i) \quad i = 1, 2, 3 \cdots n \tag{38}$$

Such that Q_i^c is the reactive power support from the shunt-connected capacitor, and its value is estimated using Eqn. (39).

$$Q_i^c = P \left[\frac{1}{pf_{(1)}} \sin\left(\cos^{-1}(pf_{(1)}) \right) - \frac{1}{pf_{(2)}} \sin\left(\cos^{-1}(pf_{(2)}) \right) \right] \tag{39}$$

Where P is the active power without capacitor compensation in the system, $pf_{(1)}$ is the uncompensated system power factor and $pf_{(2)}$ is the compensated system power factor. The equivalent capacitance requirement for the Q_i^c amount of compensation is given by Eqn. (40)

$$C = \frac{Q_C}{2\pi f V^2} \tag{40}$$

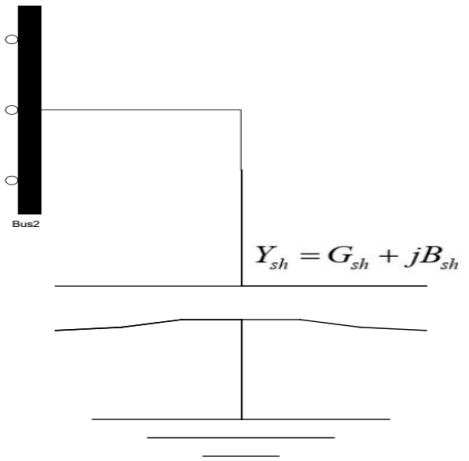

Figure 2: Model of a Shunt Capacitor connected to a bus bar

D. Hybrid Particle Swarm – Harmony Search Algorithm (PS – HSA)

The hybrid Particle Swarm – Harmony Search Algorithm (PS – HSA) combines both the exploration and exploitation capabilities of the EPS and IAHSO. While the EPSO initializes the swarm populations within the entire search space, the IAHSO modifies the individual particles turned harmonies, thereby exploiting the potentials of such solution. For an n_g generator power network, the PS – HSA objective function is implemented by Eqn. (28), while the reactive injection from the capacitor is computed by Eqn. (39). The algorithm for hybrid Particle Swarm – Harmony Search optimization is given in Table 1, while the flowchart implementation of the algorithm is given in Figure 3.

Table 1: Algorithm for Hybrid PS - HSA

Step 1	Start PSO Initialization. Generate Initial Swarm population similar. Evaluate the fitness of each member of the swarm, (PF, Power Loss and Voltage Deviation). *Start PSO's Main Loop.*
Step 2	*Start HSO Main Loop.* Transfer the Swarm particles as Harmonies with their corresponding fitness.
Step 3	Sort Harmony fitness to obtain the global (Only Power Factor is sorted as fitness criteria).
Step 4	Improvise new Harmony and evaluate its fitness (PF, Power Loss and Voltage Deviation).
Step 5	Merge Harmony and New Harmony. Update the global fitness due to merged Harmony.
Step 6	Check termination criteria for *HSO Loop*, if yes move to step 7, otherwise go to step 4. *End of HSO*
Step 7	Transfer updated Harmony into particles with their corresponding fitness. Updates particles personal best and Global Best (PF, Power Loss and Voltage Deviation)..
Step 8	Compute new velocities
Step 9	Get new particles positions with the computed velocities
Step 10	Compute the fitness of these new particle's positions
Step 11	Check termination criteria *PSO's Main Loop*, if we yes move to step 12, otherwise go to step 1.
Step 12	End of PSO

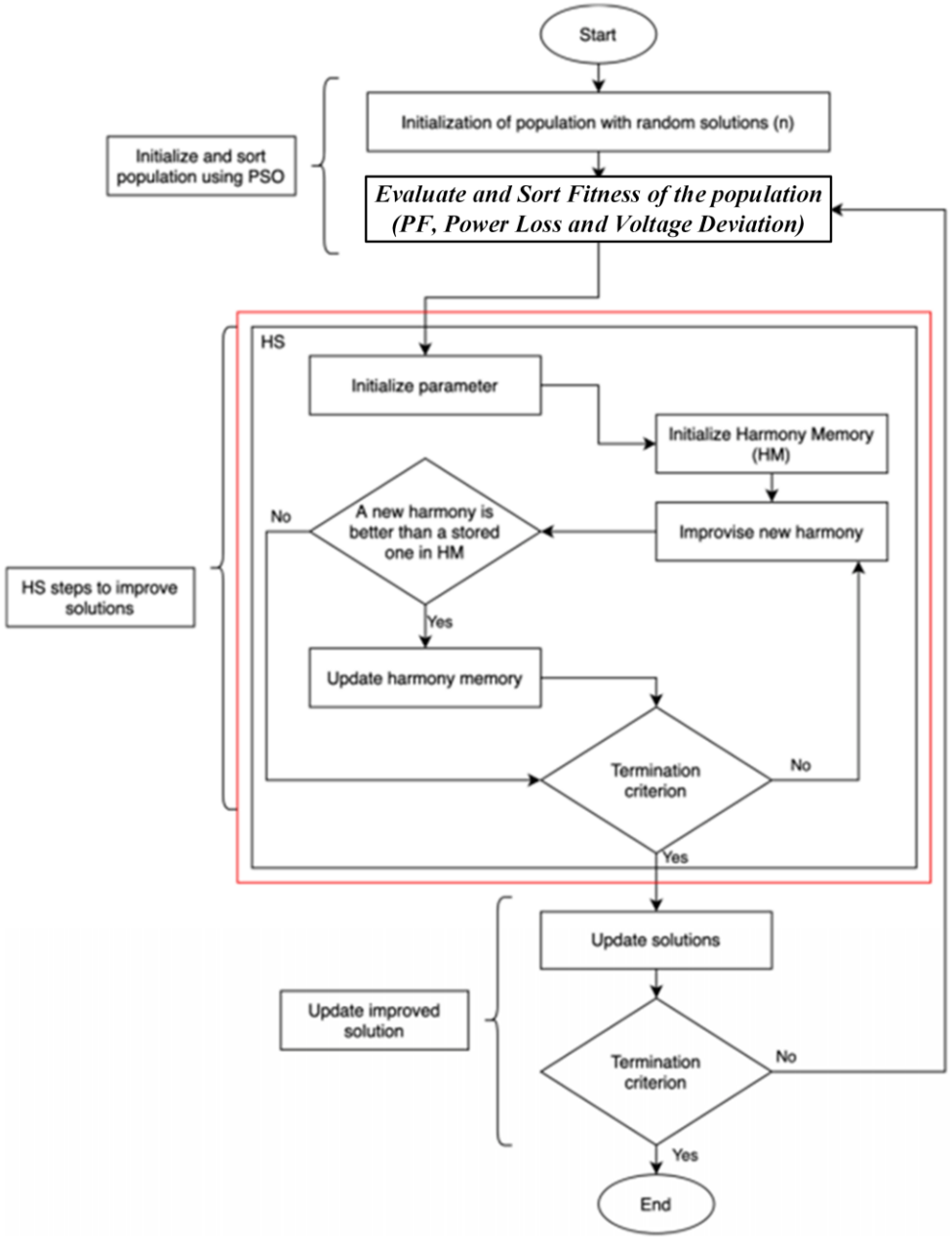

Figure 3: Flowchart for the Hybrid PS – HSA for PF Corrections

E. *Performance evaluation of IAHSO, EPSO and PS – HSA*

The various optimization techniques are evaluated in terms of the ability to obtain the optimal power factor compared to others, number of iterations to optimal solutions using their convergence characteristic curve. The results in terms of the power factor, power losses and voltage profile of each test network are compared under IAHSO, EPSO and PS – HSA. The parameters of the three optimization algorithms are documented in Table 2, where the EPSO, IAHSA and the PSO's loop of the Hybrid PS – HSA all have the same swarm sizes. For both IEEE 6 buses and IEEE 16 nodes. This will ensure a fair basis for comparison. Also, due to the search space area, in terms of the candidate location for capacitor placement, where IEEE 6 buses has 6 possible location and IEEE 16 nodes with 16 buses location, the number of iterations in each differs in accordance with the search space as indicated in Table 2. All other parameters for the HAS loop are the same.

The online diagram of the test systems in Power Systems Analysis Toolbox (PSAT) are depicted in Figures 4 and 5 for IEEE 6 buses and IEEE 16 nodes respectively.

In Figures 4 and 5, the online diagram indicates the buses or nodes where generator buses are located. In the implementation of the load flow routine and optimal capacitor planning, these buses are excluded from the search space. Additionally, for ease of reproducibility, the bus or node designated as slack is also indicated.

Table 2: Parameters of the three Optimization Algorithm

Parameters	EPSO		IAHSA		Hybrid PS – HSA	
	IEEE 6 buses	*IEEE 16 nodes*	*IEEE 6 buses*	*IEEE 16 nodes*	*IEEE 6 buses*	*IEEE 16 nodes*
Swarm Size	10	10	10	10	10	10
Max_Iter	200	2000	200	2000	PSO_loop = 100 HSA_loop = 2	PSO_loop = 100 HSA_loop = 20
C	--	--	1	1	--	--
C1	1	1	--	--	1	1
C2	4-C1	4-C1	--	--	4-C1	4-C1
W	(MaxIt - iter)/MaxIt				(MaxIt_pso - iter_pso)/MaxIt_pso;	
HMCR	--	--	0.9	0.9	0.9	0.9
HMCR_max	--	--	0.9	0.9	0.9	0.9
HMCR_min	--	--	0.6	0.6	0.6	0.6
PAR	--	--	0.3	0.3	0.3	0.3
PAR_max	--	--	0.9	0.9	0.9	0.9
PAR_min	--	--	0.01	0.01	0.01	0.01
bw	--	--	0.01	0.01	0.01	0.01
bw_max	--	--	1	1	1	1
bw_min	--	--	0.0001	0.0001	0.0001	0.0001

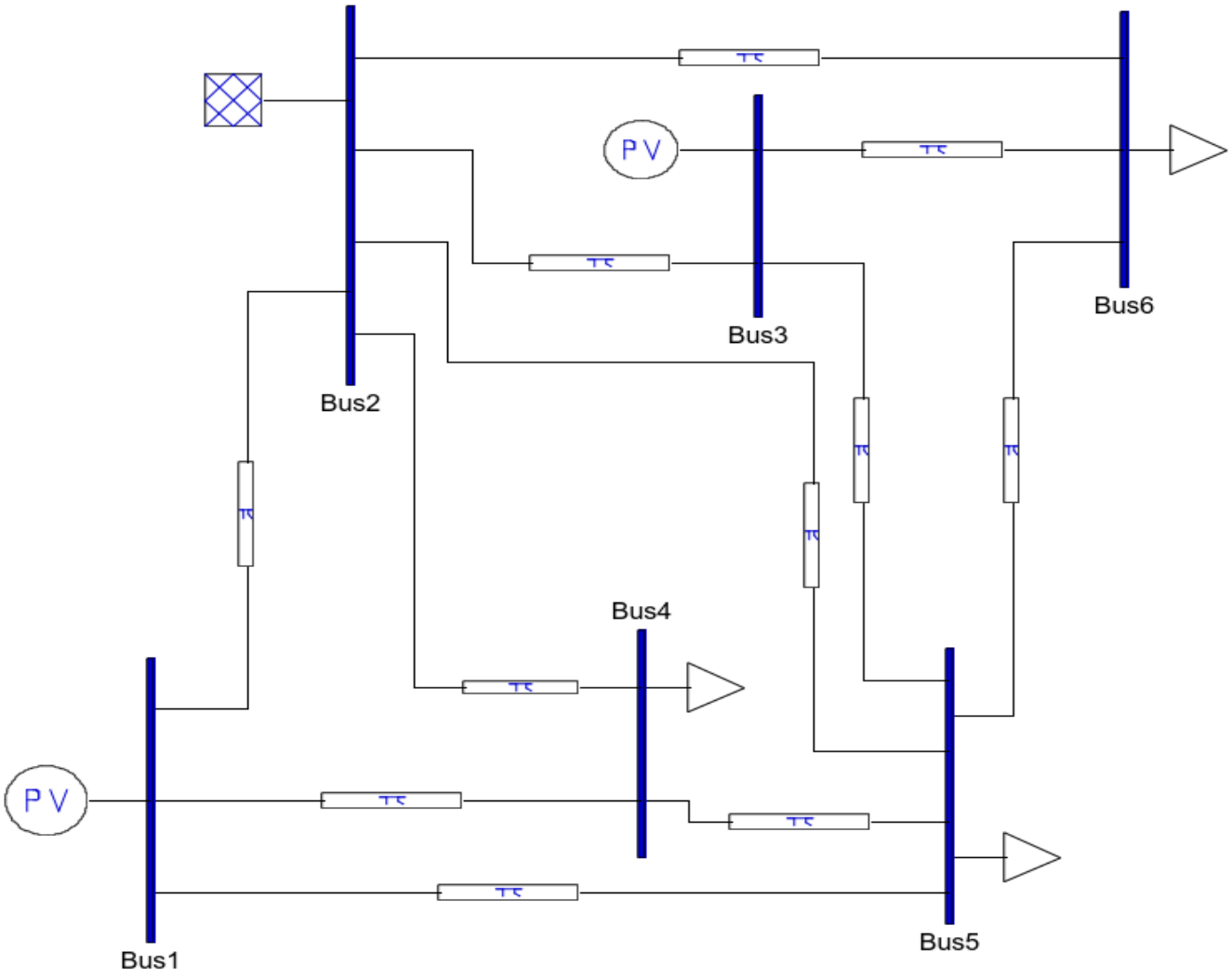

Figure 4: Modified IEEE 6 buses Model in PSAT

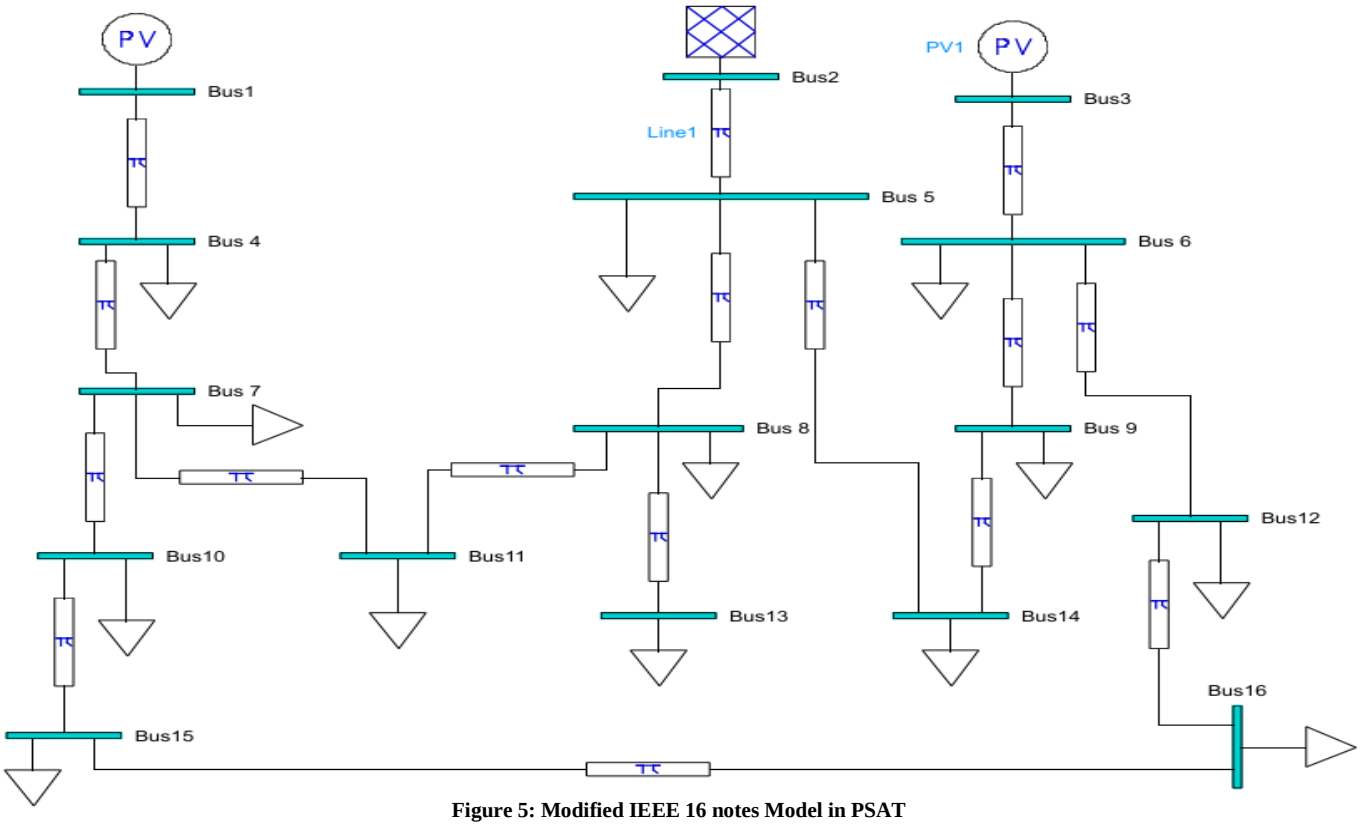

Figure 5: Modified IEEE 16 notes Model in PSAT

IV. RESULTS AND DISCUSSION

The base case pf is 0.676 and 0.76 for the IEEE 6 buses and IEEE 16 nodes respectively. Furthermore, in the base case power flow solutions, the total real power losses are 16.940 MW in IEEE 6 buses. Similarly, in the case of IEEE 16 nodes distribution network case study, the total real power loss is obtained as 0.719 MW.

A. Results of IEEE 6 Buses Transmission Network

As earlier noted, from the base case solutions of the IEEE 6 buses transmission test network, the base case power factor without capacitor placement is computed using equation (28) as 0.676. Also, the total power loss is obtained as 16.94 MW. The implementation of the three algorithms is therefore targeted at maximization of the power factor pf.

B. Optimal Capacitor Placement in IEEE 6 Buses using EPSO

Upon the execution of the EPSO for optimal capacitor placement in IEEE 6 buses network for pf correction, the pf was improved from the base case value of 0.676 to 0.8981 as depicted in Figure 6. It is observed from Figure 6 that the pf with EPSO converges after about 74 iterations, while the mean value, which indicates the number of iterations where all members of the swarm reached the same optimal pf of 0.898 is after 161 iterations.

C. Optimal Capacitor Placement in IEEE 6 Buses using IAHSA

In the case of IAHSA, Figure 7 shows the convergence curve where one of the harmonies obtained the optimal pf of 0.898 after 67 iterations and the mean which indicates the number of iterations where all members of the harmony memory reached the optimal pf is after 95 iterations.

D. Optimal Capacitor Placement in IEEE 6 Buses using Hybrid PS – HAS

For the hybrid PS – HSA, the convergence characteristics is depicted in Figure 8. In other to ensure fair comparison, the hybrid PS – HSA convergence curve is plotted for the entire iteration loop which can be computed from Table 2, that is; 100 iterations of the PSO's loop multiplied by 2 iterations of the HSA loop, gives 200 iterations. Consequently, from Figure 8, the hybrid PS – HSA converges after just about 12 iterations while the mean for all members of the harmonies and swarm reached the optimal pf after 77 iterations.

The performance of the three algorithms EPSO, IAHSA and hybrid PS – HSA in terms of the convergence characteristics are depicted in Figure 9.

E. Optimal Capacitor Placement in IEEE 16 Nodes Distribution Network

Similar to the results of the IEEE 6 buses, the base case solutions of the IEEE 16 nodes distribution test network are also obtained. The base case power factor without capacitor is equally computed using Eqn. (28), as 0.76. Also, the total power loss is obtained as 0.719 MW. The three algorithms are executed with maximization of the power factor pf as objective function.

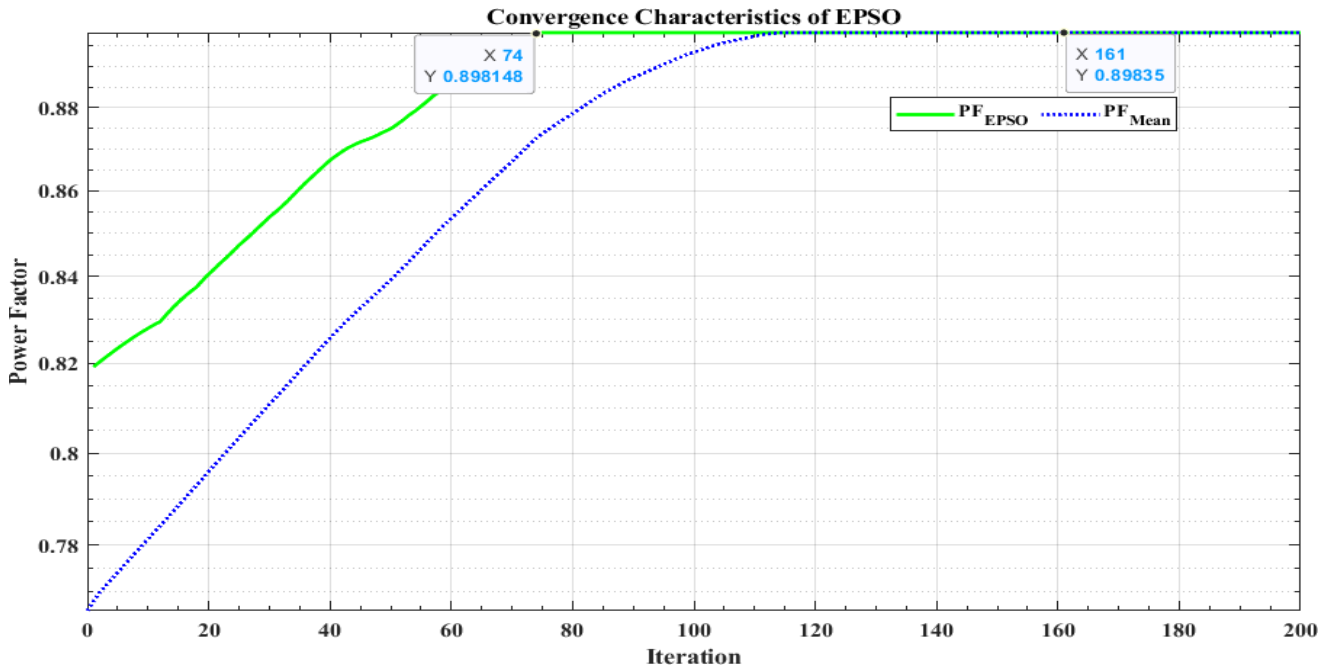

Figure 6: Convergence characteristics of EPSO for IEEE 6 buses

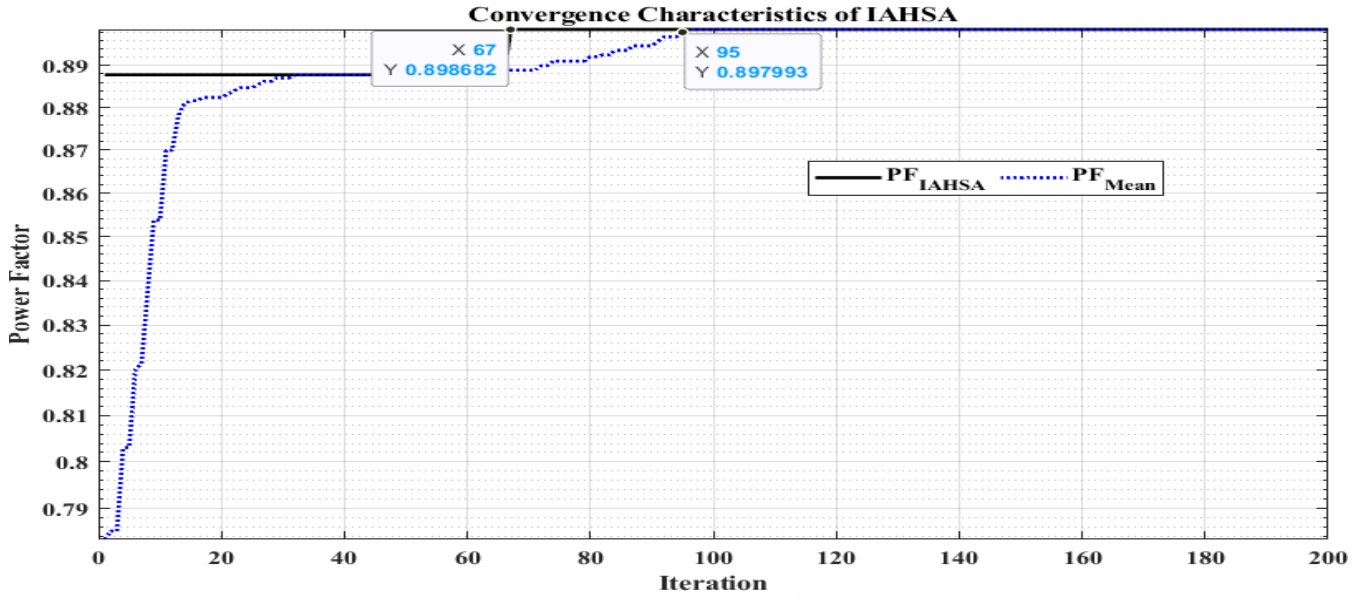

Figure 7: Convergence characteristics of IAHSA for IEEE 6 buses

F. Optimal Capacitor Placement in IEEE 16 Nodes using EPSO

After the maximum number of 2000 iterations of the EPSO for optimal capacitor placement in IEEE 16 buses for power factor (pf) correction, the pf was improved from the base case value of 0.76 to 0.9439 as depicted in Figure 10. From this figure, the pf with EPSO converges after about 597 iterations, while the mean value, indicating the number of iterations at which all members of the swarm reached the same optimal pf of 0.88439 is after 1575 iterations.

G. Optimal Capacitor Placement in IEEE 16 Nodes using IAHSA

The convergence characteristics of IAHSA in the case of IEEE 16 nodes distribution test network is given in Figure 11. It is observed that the IAHSA obtained the optimal pf of 0.9427 after 1795 iterations, while the mean pf for all members of the harmony memory is obtained at 1848 iterations.

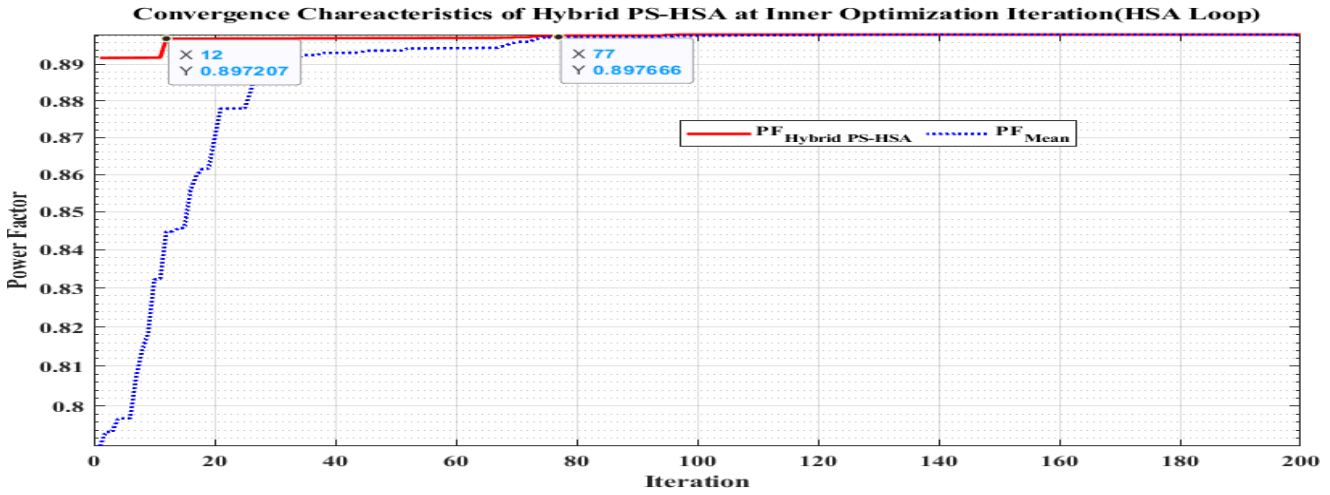

Figure 8: Convergence characteristics of Hybrid PS – HSA IEEE 6 buses

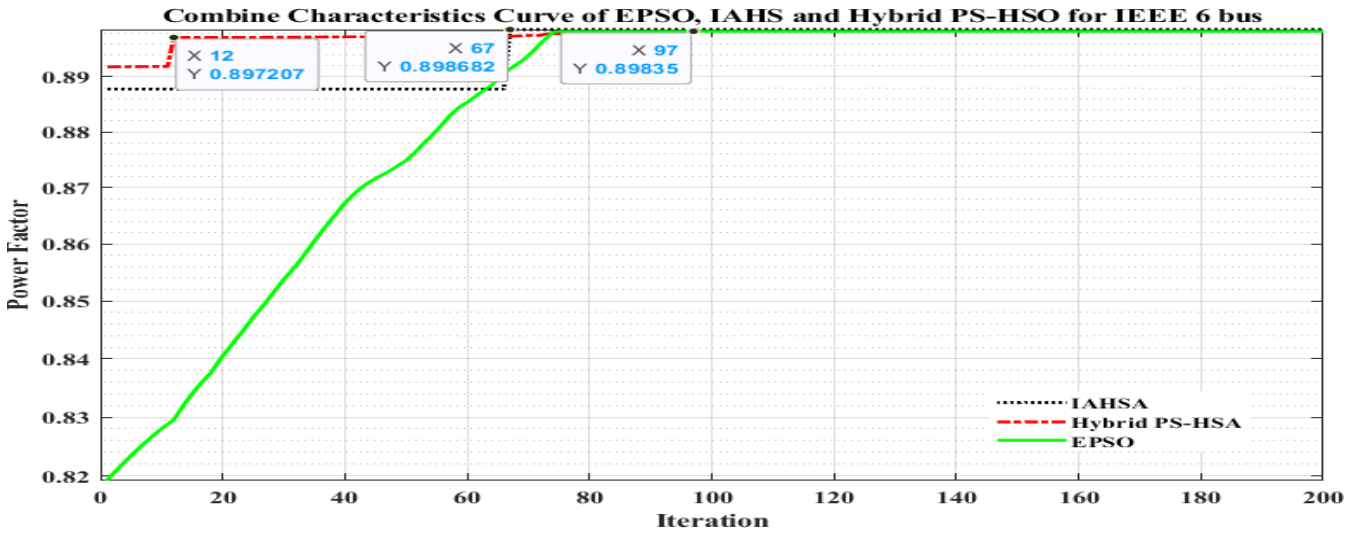

Figure 9: Performance comparison of EPSO, IAHS and Hybrid PS-HSO under IEEE 6 transmission network.

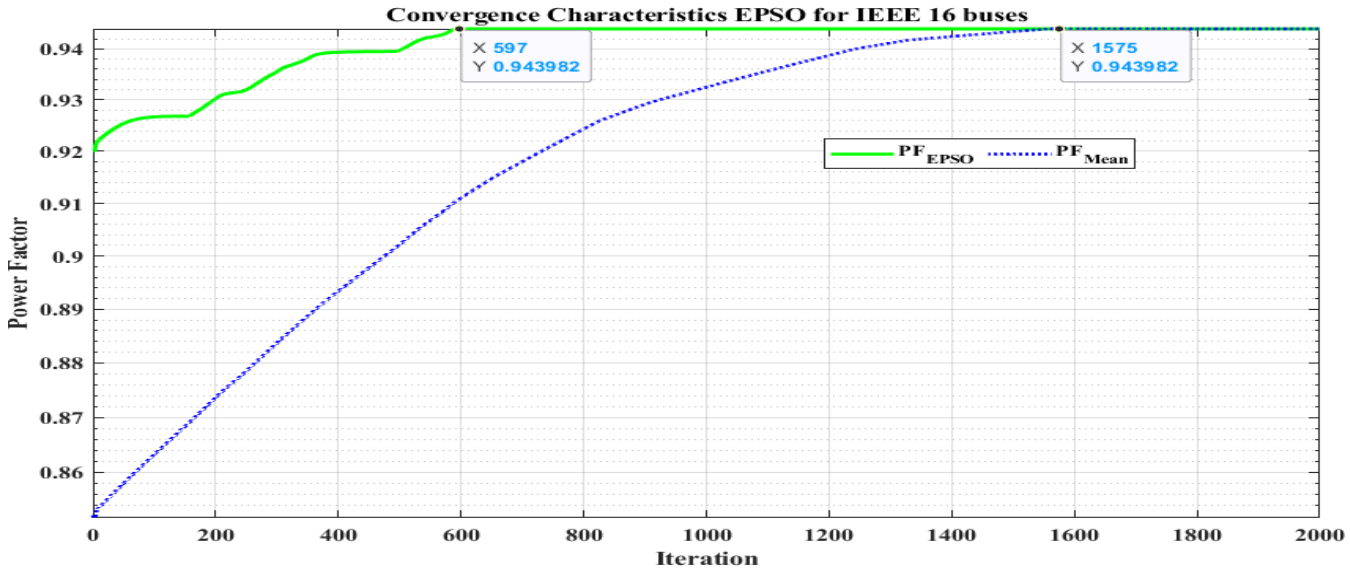

Figure 10: Convergence characteristics of EPSO for IEEE 16 buses

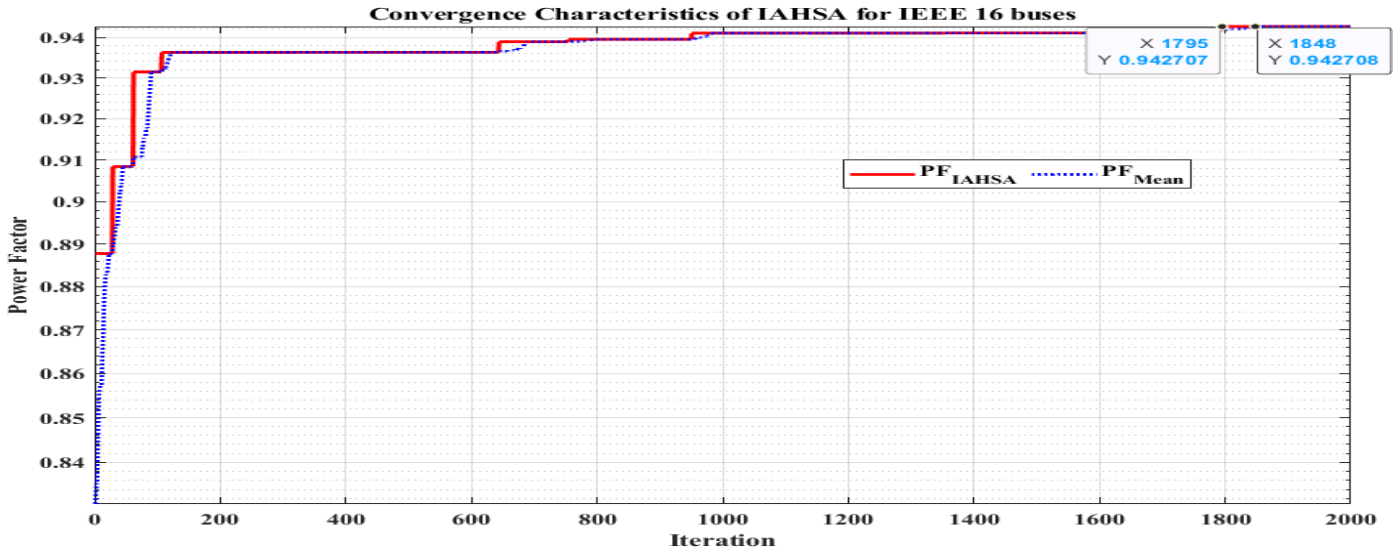

Figure 11: Convergence characteristics of IAHSA for IEEE 16 nodes

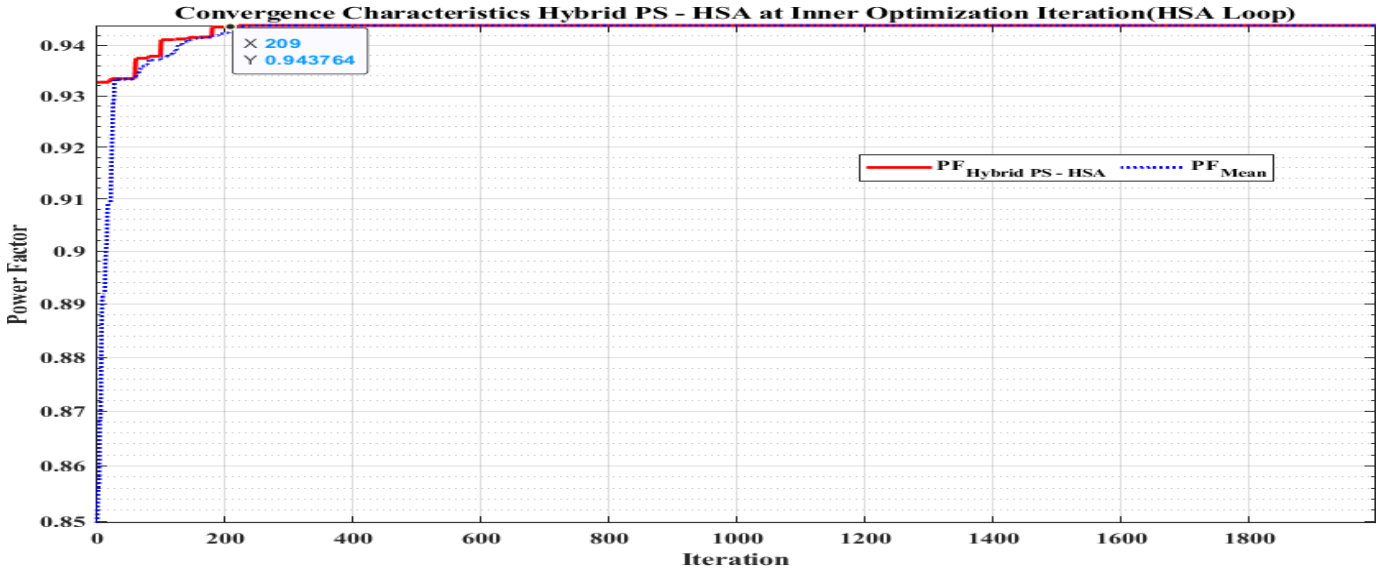

Figure 12: Convergence characteristics of Hybrid PS - HSA for IEEE 16 nodes

H. Optimal Capacitor Placement in IEEE 16 Nodes using Hybrid PS – HSA

In the same vein, the convergence curve of the hybrid PS – HSA is depicted in Figure 12, and the optimal pf obtained is 0.9437 at about 209 iterations. It is observed that both the optimal pf and the mean of all members of the harmonies and swarm reached the optimal pf after approximately equal number of iterations. This is despite the starting point for the optimal pf which is above 0.93 and the mean pf at 0.85, as indicated in Figure 12.

Furthermore, the performance comparison of the three algorithms: EPSO, IAHSA and hybrid PS – HSA under IEEE 16 nodes distribution network are depicted in Figure 13. For both modified IEEE 6 buses transmission network and IEEE 16 nodes distribution network, all the three algorithms were able to maximize the system power factor. In the case of the modified IEEE 6 buses, the improvement in pf is from 0.676 to 0.8981, 0.8986 and 0.898 for EPSO, IAHSA and hybrid PS – HSA respectively. The EPSO, IAHSA and hybrid PS – HSA achieved the optimal pf after 74, 67 and 12 iterations respectively. Figure 14 depicts the performance comparison in terms of the number of iterations to convergence. From Figure 14, it is evident that the proposed hybrid PS – HSA outperforms both EPSO and IAHSA with lower number of iterations to convergence.

Similarly, in the case of IEEE 16 nodes distribution network, Figure 15 depicts the performance comparison in terms of the number of iterations to convergence, and it is shown again that the proposed hybrid PS – HSA outperforms both EPSO and IAHSA with lower number of iterations to convergence. Therefore, the hybrid PS – HSA performs better both in transmission and distribution network.

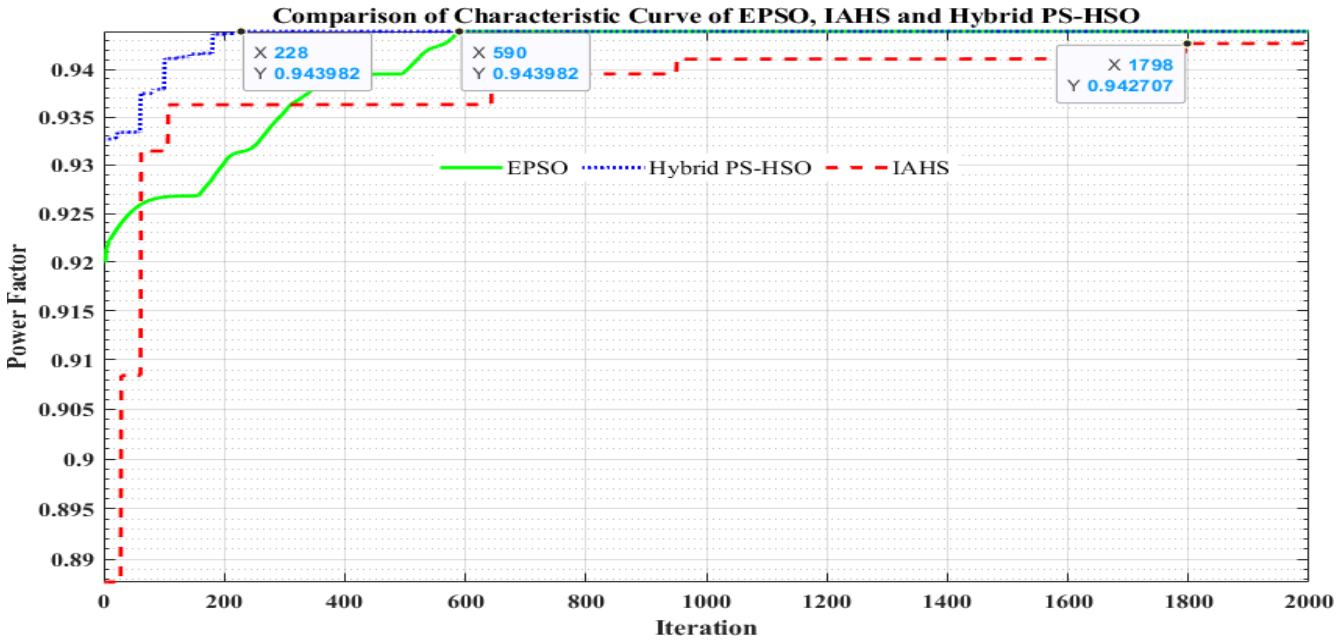

Figure 13: Performance comparison of the convergence curves for EPSO, IAHS and Hybrid PS-HSO under IEEE 16 nodes distribution Network.

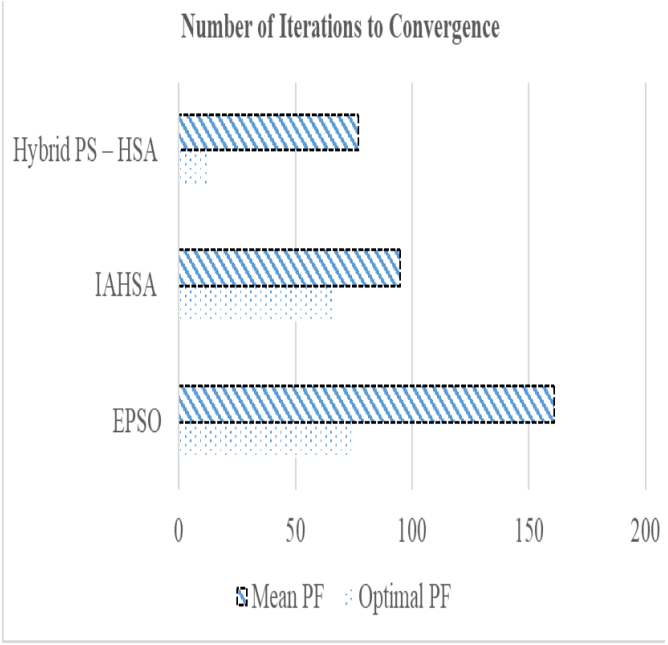

Figure 14: Comparisons of EPSO, IAHSA and Hybrid PS – HSA under IEEE 6 buses.

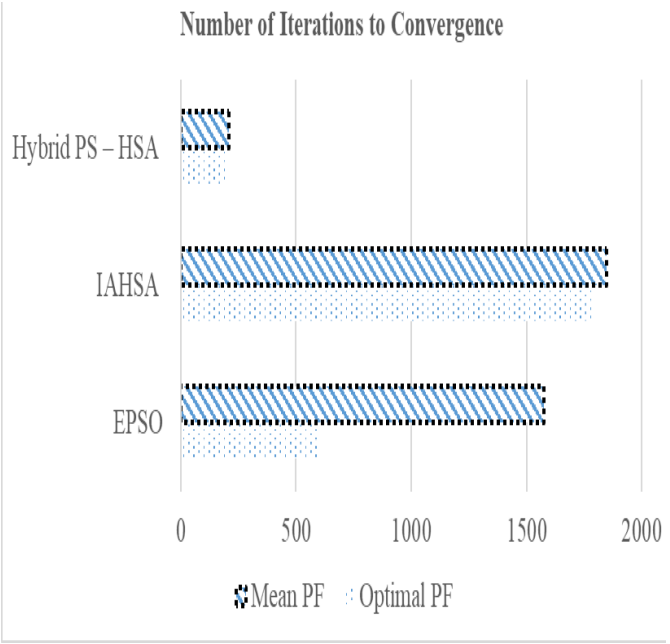

Figure 15: Comparisons of EPSO, IAHSA and Hybrid PS – HSA for IEEE 16 nodes.

I. Impacts of Capacitor Placement on Real Power Loss Reduction

Although this research focuses on the optimal capacitor placement for power factor correction, its impact on real power loss minimization is also investigated. Consequently, the line losses for each test network are obtained before and after placement of the capacitor at the optimally obtained bus or node obtained by the hybrid PS – HSA.

Figure 16 shows the comparison between base case real power loss and the losses after optimal placement of capacitors in IEEE 6 buses transmission network. At the base case and without capacitor, the total power loss is about 16.94 MW, and upon placement of capacitor for power factor correction, the real power loss decreases to 14.03 MW, this account for 17.2% reduction in real power loss.

Similarly, Figure 17 shows the comparison between the base case real power losses and the power losses after capacitor placement for power factor correction under the IEEE 16 nodes distribution network. As compared to the base case with total power loss of 0.719 MW, the optimal capacitor placement also achieved a reduction of real power loss to 0.69 MW. This results in about 4% reduction in power loss.

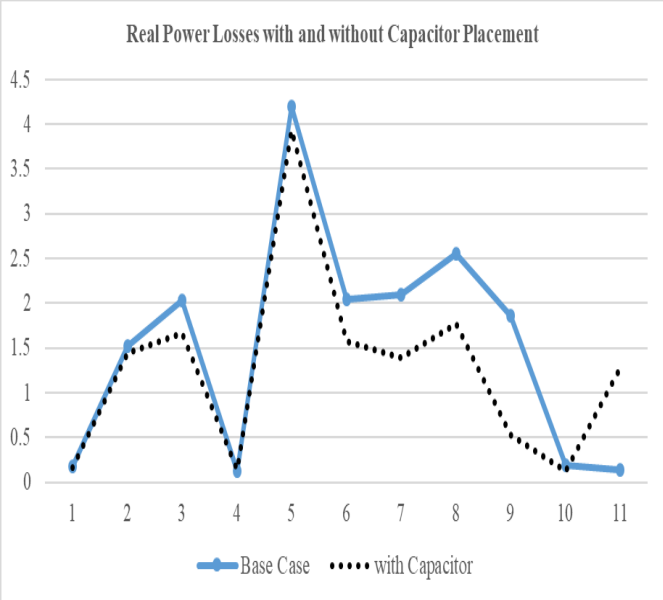

Figure 16: Real power loss with/without capacitor optimal placement for IEEE 6

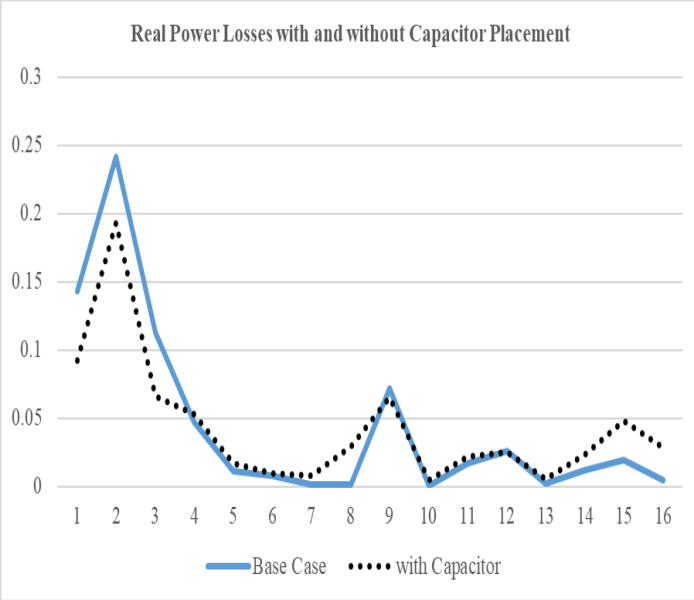

Figure 17: Real power loss with/without capacitor optimal placement for IEEE 16.

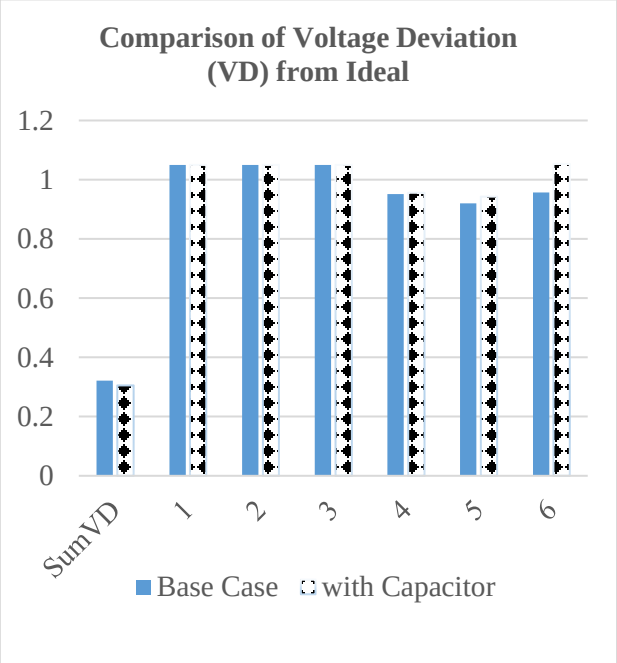

Figure 18: Voltage Deviations with/without Capacitor for IEEE 6 buses.

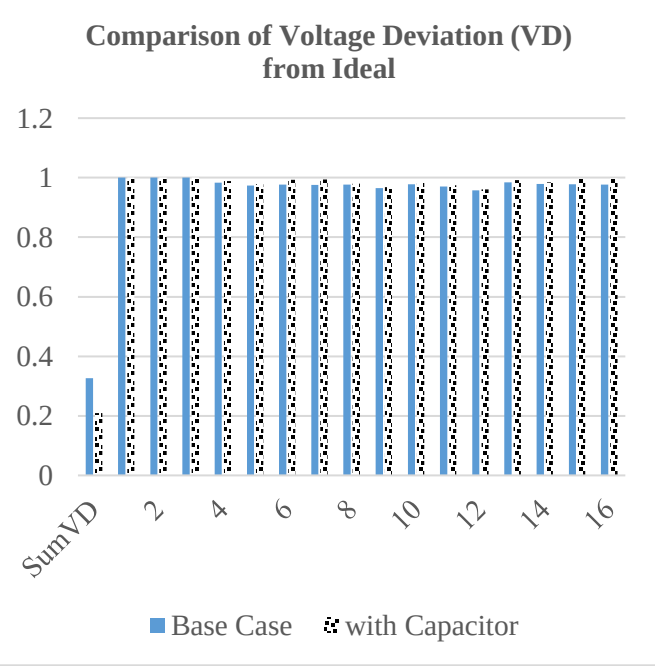

Figure 19: Voltage Deviations with/without Capacitor for IEEE 16 nodes.

J. Impacts of Capacitor Placement on Voltage Deviation

Similarly, after optimal capacitor placement and sizing for power factor corrections, the impacts of the capacitor on voltage deviation at PQ buses are investigated. Consequently, Figure 18 shows that the bus 5 voltage magnitude of IEEE 6 buses, improves from 0.92 p.u., to about 0.943 p. u, and the sums of the deviation of the voltage away from 1p.u., reduces from 0.3214 to 0.3050.

Similar trend is also observed for the case of IEEE 16 nodes as depicted in Figure 19, where it is observed that nodes 4 to 16 all improves in magnitude due to MVAR injection from capacitor. The deviation of voltage decreases from 0.3267p.u., in the base case to 0.2098 after optimal capacitor placement in the IEEE 16 nodes network.

Table 3 gives the detailed solution of the locations and sizes of the optimal capacitor placement for power factor correction in both the modified IEEE 6 and 16 buses and nodes respectively.

Table 3: Optimal Capacitor Solutions for both IEEE 6 buses and IEEE 16 nodes.

IEEE 6 Buses	EPSO	IAHSA	Hybrid PS – HSA
Location (Bus no.)	6	5	6
Size [MVAR]	150	149.665	150
PF	0.8983	0.8986	0.8992
Base Case PF	0.68	0.68	0.68
IEEE 16 Nodes			
Location (Bus no.)	16	15	16
Size [MVAR]	14.999	14.989	14.999
PF	0.9439	0.943	0.944
Base Case PF	0.76	0.76	0.76

The impacts of optimal capacitor placement on both power loss and volage deviation with the objective of power factor correction were discussed. Although the capacitor placement and sizing objective centered on power factor improvement, this optimal placement also improves the power loss and voltage deviation of both test networks. Additionally, a validation on the size of capacitor was carried out in comparison with the theoretical MVAR requirement to improve the power factor. It was also observed that the MVAR obtained by the optimization algorithms were within range of the theoretical MVAR requirements calculated for both test networks.

V. CONCLUSION

In this research work, the standard IEEE 6 buses and IEEE 16 nodes test networks were modified to clearly depict an inductive load dominated power system; thereby modelling heavy presence of industrial loads. This is evident in the poor power factor recorded in both systems: 0.68 and 0.76 respectively. A Hybrid Particle Swarm and Harmony Search Algorithm (PS – HSA) was developed to improve power factor of each test network measured from the source end. Optimal location and size of the capacitors in the IEEE 6 buses and IEEE 16 nodes were bus 6 with 150 MVAR injections, and node 16 with 14.99 MVAR injections respectively. The EPSO, IAHSA and hybrid PS – HSA achieved the optimal pf after 74, 67 and 12 iterations respectively. The Improved quantitative power factor obtained are 0.8992 and 0.944 for IEEE 6 buses and IEEE 16 buses respectively with the hybrid PS – HSA. This improvement in real power utilization is attributed to the optimal capacitor sizing and location. These said improvement translate to 32% and 24% percentage improvement in power factor for IEEE 6 buses and IEEE 16 nodes, compared to the base case, respectively. The optimal planning of capacitors increases the efficiency of the power system in terms of minimization of power losses and voltage profile in the tested networks which were earlier dominated with inductive load. The efficiency is quantitatively measured as 17.2% and 4% reduction in power losses for IEEE 6 buses and IEEE 16 nodes respectively. Similarly, the improvement in voltage deviation indicates from 0.3214 to 0.3050 for IEEE 6 buses and from 0.3267 to 0.2098 in the case of IEEE 16 nodes.

AUTHOR CONTRIBUTIONS

A. H, Ibrahim: Conceptualization, Software and Simulation, Validation, Writing – original draft. **E. C. Ashigwuike:** Conceptualization, Methodology, Supervision. **W. Oluyombo:** Supervision Writing – review & editing. **A. A. Sadiq:** Software, Simulation and Writing – review & editing.

REFERENCES

B. -J. Huang (2018). 'Interleaved Voltage-Doubler Boost Converter for Power Factor Correction', in *2018 International Power Electronics Conference (IPEC-Niigata 2018 -ECCE Asia),*. Niigata, Japan, pp. 3528–3532. doi: 10.23919/IPEC.2018.8507419.

Balu, K. and Mukherjee, V. (2020). 'Siting and Sizing of Distributed Generation and Shunt Capacitor Banks in Radial Distribution System Using Constriction Factor Particle Swarm Optimization', *Electric Power Components and Systems*, 48(6–7), pp. 697–710. doi: 10.1080/15325008.2020.1797935.

Beck, K. (2018). Types of Electrical Loads. Available at: https://sciencing.com/types-electrical-loads-8367034.html on 9th October 2021. (Accessed: 9 October 2021).

Blume, S. W. (2007). *Electric Power System Basics*. Edited by M. E. El-Hawary. NJ: IEEE Press.

Bouaraki, M. and Recioui, A. (2017). 'Optimal placement of power factor correction capacitors in power systems using Teaching Learning Based Optimization', *ALGERIAN JOURNAL OF SIGNALS AND SYSTEMS (AJSS) Optimal*, 2(2), pp. 102–109. doi: https://doi.org/10.51485/ajss.v2i2.37.

Che Soh, S., Hasim, H., As, A. A., Teknikal, B. S., & Malaysia, A. N. (2014) 'Impact Study on Power Factor of Electrical Load in Power Distribution System', *R&D Seminar 2014: Research and Development Seminar 2014, Malaysia*, pp. 1–8. Available at: https://inis.iaea.org/search/search.aspx?orig_q=RN:46091351 .

Chen, G., Zhang, J. and Taleb Ziabari, M. (2022). 'Optimal allocation of capacitor banks in distribution systems using particle swarm optimization algorithm with time-varying acceleration coefficients in the presence of voltage-dependent loads', *Australian Journal of Electrical and Electronics Engineering*, 19(1), pp. 87–100. doi: https://doi.org/10.1080/1448837X.2021.2023075.

Elsheikh, A., Helmy, Y., Abouelseoud, Y., & Elsherif, A. (2014) 'Optimal capacitor placement and sizing in radial electric powe r systems', *Alexandria Engineering Journal*, 53(4), pp. 809–816. doi: 10.1016/j.aej.2014.09.012.

Eswaran, T. and Kumar, V. S. (2017). 'Particle swarm optimization (PSO)-based tuning technique for PI controller for management of a distributed static synchronous compensator (DSTATCOM) for improved dynamic response and power quality', *Journal of Applied Research and Technology*, 15(2), pp. 173–189. doi: 10.1016/j.jart.2017.01.011.

Gampa, S. R. and Das, D. (2016). 'Optimum placement of shunt capacitors in a radial distribution system for substation power factor improvement using fuzzy GA method', *International Journal of Electrical Power and Energy Systems*, 77, pp. 314–326. doi: 10.1016/j.ijepes.2015.11.056.

García, O., Cobos, J. A., Prieto, R., Alou, P., & Uceda, J. (2003) 'Single phase power factor correction: A survey', *IEEE Transactions on Power Electronics*, 18(3), pp. 749–755. doi: 10.1109/TPEL.2003.810856.

Hussain, A. N.; A. A. Abdullah and O. M. Neda. (2018). 'Modified Particle Swarm Optimization for Solution of Reactive Power Dispatch', *Research Journal of Applied Sciences, Engineering and Technology*, 15(8), pp. 316–327. doi: 10.19026/rjaset.15.5917.

Iza, L. E. F.; M. D. J. Monge and W. D. P. Vallejos. (2022). 'Power factor improvement through optimal placement and sizing of D-STATCOM using particle swarming optimization', in *In 2022 International Conference on Electrical, Computer, Communications and Mechatronics Engineering (ICECCME)*. Maldives: IEEE, pp. 1–6. doi: 10.1109/ICECCME55909.2022.9988157.

Khadhraoui, T., Ktata, S., Benzarti, F., & Amiri, H (2016) 'Features Selection Based on Modified PSO Algorithm for 2D Face Recognition', in *Proceedings - Computer Graphics, Imaging and Visualization: New Techniques and Trends, CGiV 2016*, pp. 99–104. doi: 10.1109/CGiV.2016.28.

Kumar, R. (2022). 'Fuzzy particle swarm optimization control algorithm implementation in photovoltaic integrated shunt active power filter for power quality improvement using hardware-in-the-loop', *Sustainable Energy Technologies and Assessments*, 50(101820). doi: https://doi.org/10.1016/j.seta.2021.101820.

Lasseter, R. H., Eto, J. H., Schenkman, B., Stevens, J., Vollkommer, H., Klapp, D., Linton, E., Hurtado, H., & Roy, J (2011) 'CERTS microgrid laboratory test bed', *IEEE Transactions on Power Delivery*, 26(1), pp. 325–332. doi: 10.1109/TPWRD.2010.2051819.

Lotfi, H.; M. B. Elmi and S. Saghravanian. (2018) 'Simultaneous placement of capacitor and DG in distribution networks using particle swarm optimization algorithm', *International Journal of Smart Electrical Engineering*, 7(1), pp. 35–41.

Mahmoud, R. A. A. and Emam, A. (2022). 'Coherence-based automatic power factor correction (APFC) algorithm for power grids', *The Journal of Engineering*, 2022(5), pp. 512–527. doi: 10.1049/tje2.12133.

Mehta, V. K. and Mehta, R. (2008). Principles of electrical machines. New Delhi: S. Chand Publishing. Available at: https://books.google.com.ng/books?hl=en&lr=&id=JLQn1AHdzxsC&oi=fnd&pg=PR1&dq=Mehta,+V.+K.+and+Mehta,+R.+(2005).+Principle+of+Electrical+Machines&ots=JmRieHpn_A&sig=LQJqXo5A4RslszfbbXCq5oWHQRE&redir_esc=y#v=onepage&q&f=false.

Mendoza, G. E.; V. M. Vacas and N. R. Ferreira. (2019). 'Optimal Capacitor Allocation and Sizing in Distribution Networks Using Particle Swarm Optimization Algorithm', *WCNPS 2018 - Workshop on Communication Networks and Power Systems*, pp. 1–5. doi: 10.1109/WCNPS.2018.8604320.

Mohammadi, M. (2017). 'Particle swarm optimization algorithm for simultaneous optimal placement and sizing of shunt active power conditioner (APC) and shunt capacitor in harmonic distorted distribution system', *Journal of Central South University*, 24(9), pp. 2035–2048. doi: 10.1007/s11771-017-3613-7.

Naderi, E., Narimani, H., Fathi, M., & Narimani, M. R. (2017) 'A novel fuzzy adaptive configuration of particle swarm optimization to solve large-scale optimal reactive power dispatch', *Applied Soft Computing Journal*, 53, pp. 441–456. doi: 10.1016/j.asoc.2017.01.012.

Neupane, D., Poudel, B., Khatri, N., Yadav, D., & Khadka, D. (2020) 'Optimal Capacitor Placement using Particle Swarm Optimisation (PSO): A Case Study in 33kV Distribution System', (September), pp. 121–126.

Ospina, L. D. P. and Van Cutsem, T. (2020). 'Power factor improvement by active distribution networks during voltage emergency situations', in *21st Power Systems Computation Conference PSCC2020*. Porto, Portugal, pp. 1–8. doi: 10.1016/j.epsr.2020.106771.

Prasetyo, Y., Hidayatullah, N. A., Artono, B., & Danu S, B. (2021) 'Power Factor Correction Using Programmable Logic Control Based Rotary Method', *Journal of Physics: Conference Series*, 1845(1). doi: 10.1088/1742-6596/1845/1/012045.

Qiao, J.; C. Wang and J. Wei. (2015) 'An adaptive particle swarm optimization algorithm with local search', *Information and Control*, 44(4), pp. 385–392. doi: 10.13976/j.cnki.xk.2015.0385.

Qin, S., Lei, Y., Ye, Z., Chou, D., & Pilawa-Podgurski, R. C. N. (2019) 'A High-Power-Density Power Factor Correction Front End Based on Seven-Level Flying Capacitor Multilevel Converter', *IEEE Journal of Emerging and Selected Topics in Power Electronics*, 7(3), pp. 1883–1898. doi: 10.1109/JESTPE.2018.2865597.

Ramadan, H. S.; A. F. Bendary and S. Nagy. (2017) 'Particle swarm optimization algorithm for capacitor allocation problem in distribution systems with wind turbine generators', *International Journal of Electrical Power and Energy Systems*, 84, pp. 143–152. doi: 10.1016/j.ijepes.2016.04.041.

Sajjadi, S. M.; M. R. Haghifam and J. Salehi. (2013). 'Simultaneous placement of distributed generation and capacitors in distribution networks considering voltage stability index', *International Journal of Electrical Power and Energy Systems*, 46(1), pp. 366–375. doi: 10.1016/j.ijepes.2012.10.027.

Subjak, J. S. and Mcquilkin, J. S. (1990). 'Harmonies—Causes, Effects, Measurements, and Analysis: An Update', *IEEE Transactions on Industry Applications*, 26(6), pp. 1034–1042. doi: 10.1109/28.62384.

Tahir, M. J.; M. B. Rasheed and M. K. Rahmat. (2022). 'Optimal Placement of Capacitors in Radial Distribution Grids via Enhanced Modified Particle Swarm Optimization', *Energies*, 15(7), pp. 1–27. doi: 10.3390/en15072452.

Yapici, H. and Çetinkaya, N. (2017). 'An Improved Particle Swarm Optimization Algorithm Using Eagle Strategy for Power Loss Minimization', *Mathematical Problems in Engineering*, 2017. doi: 10.1155/2017/1063045.

Yoshida, H. and Fukuyama, Y. (2018). 'Parallel Multipopulation Differential Evolutionary Particle Swarm Optimization for Voltage and Reactive Power Control', *Electrical Engineering in Japan (English translation of Denki Gakkai Ronbunshi)*, 204(3), pp. 31–40. doi: 10.1002/eej.23100.

Zimmerman, R. D.; C. E. Murillo-Sanchez and R. J. Thomas. (2011). 'MATPOWER: Steady-State Operations,

Planning, and Analysis Tools for Power Systems Research and Education', *IEEE Transactions on Power Systems*, 26(1), pp. 12–19. doi: 10.1109/TPWRS.2010.2051168.

Zou, L. (2021). 'Design of reactive power optimization control for electromechanical system based on fuzzy particle swarm optimization algorithm', *Microprocessors and Microsystems*, 82(December 2020), p. 103865. doi: 10.1016/j.micpro.2021.103865.